# Accepted Manuscript

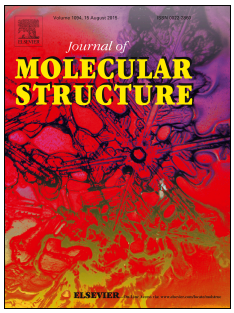


Thermal decomposition and vibrational spectroscopic aspects of pyridinium hexafluorophosphate ($C_5H_5NHPF_6$)

M.D.S. Lekgoathi, L.D. Kock

PII: S0022-2860(16)30665-2

DOI: 10.1016/j.molstruc.2016.06.078

Reference: MOLSTR 22697

To appear in: *Journal of Molecular Structure*

Received Date: 22 December 2015

Revised Date: 28 June 2016

Accepted Date: 28 June 2016

Please cite this article as: M.D.S. Lekgoathi, L.D. Kock, Thermal decomposition and vibrational spectroscopic aspects of pyridinium hexafluorophosphate ($C_5H_5NHPF_6$), *Journal of Molecular Structure* (2016), doi: 10.1016/j.molstruc.2016.06.078.

## Graphical Abstract

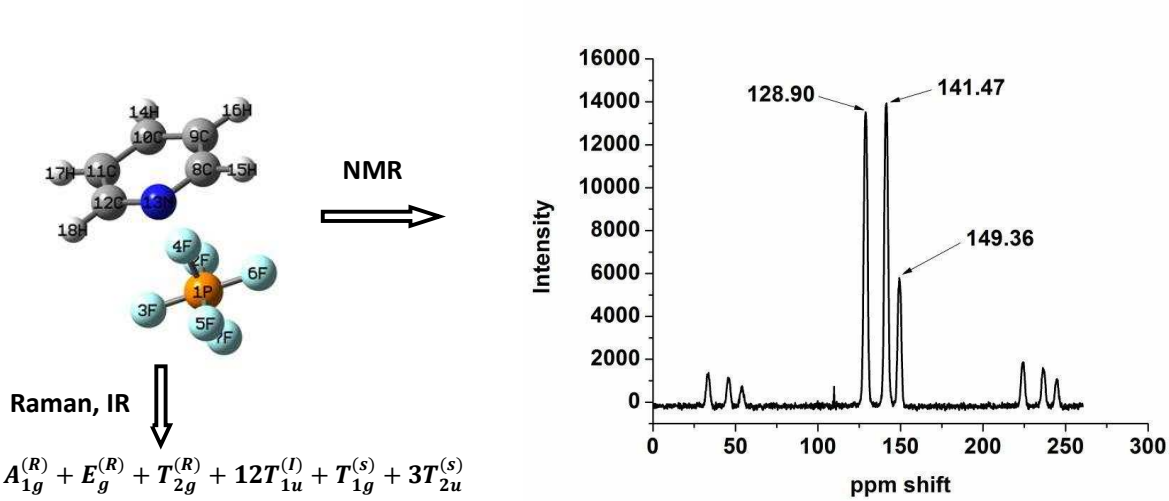

# Thermal decomposition and vibrational spectroscopic aspects of Pyridinium Hexafluorophosphate ($C_5H_5NHPF_6$)

**M.D.S. Lekgoathi**[*†]**,L.D. Kock**[†].

[†]Department of Applied Chemistry, South African Nuclear Energy Corporation SOC Limited (Necsa), P.O. Box 582, Pretoria 0001, South Africa.

## Abstract

Thermal decomposition and vibrational spectroscopic properties of pyridinium hexafluorophosphate ($C_5H_5NHPF_6$) have been studied. The structure of the compound is better interpreted as having a cubic space group, based on Raman and infrared vibrational spectroscopy experiments and group theoretical correlation data between site symmetry species and the spectroscopic space group. The $^{13}C$ NMR data shows three significant signals corresponding to the three chemical environments expected on the pyridinium ring i.e. γ, β and α carbons, suggesting that the position of the anion must be symmetrical with respect to the pyridinium ring's $C_{2v}$ symmetry. The process of thermal decomposition of the compound using TGA methods was found to follow a contracting volume model. The activation energy associated with the thermal decomposition reaction of the compound is 108.5 kJ.mol$^{-1}$, while the pre exponential factor is 1.51 x $10^9$ sec$^{-1}$.

**Key words**: Pyridinium hexafluorophosphate, Group theory, Raman, TGA, Kinetics

[*]Corresponding author: M.D.S Lekgoathi, Tel: +27 12 305 6839 Fax: +27 12 305 6945.
E-mail: mpho.lekgoathi@necsa.co.za

# 1. Introduction

Pyridinium hexafluorophosphate is a well-known precursor used in the synthesis of metal hexafluorophosphate salts [1]. These salts find applications as components of inhibitors, polymerization catalysts and flame retardants, but most importantly, in rechargeable batteries (lithium, potassium and sodium ion-batteries). The vibrational spectroscopic properties of pyridinium hexafluorophosphate have been studied before [1,2], but no mention of its thermal decomposition signature has been made and no correlation of vibrational spectroscopy experimental data with group theory was made to seek agreement and structural consistency with the space group for this important compound. It is possible to misinterpret vibrational spectroscopy data of a compound if the underlying space group is not verified by correlating Raman and IR experimental data with group theory [3]. For example, It has been shown that for the $LiPF_6$ salt, Raman spectroscopy is a much more sensitive probe in situations where order/disorder or phase transition processes occur [4], a blind spot for pXRD. Phase transitions associated with order-disorder orientations in the pyridinium ring have also been observed for pyridinium hexafluorophosphate ($C_5H_5NHPF_6$) and related compounds [5]. This is in contrast with the works of Copeland *et al*. [6], who could not observe any associated phase transitions for the same compound, and concluded that there is only one crystal structure for $C_5H_5NHPF_6$, being *R-3m (166)*. However, the works of Cook [7], on the vibrational spectroscopy of pyridinium salts show that the pyridinium ring itself has a $C_{2v}$ symmetry, and when interpreted from the perspective of $C_5H_5NHPF_6$, we should expect the presence of several triply degenerate phonon modes as part of the irreducible representations of the compound, emanating from the octahedral $PF_6^-$ anion.

The structural data for a particular material has a strong dependence on the local symmetry of that material. Vibrational spectroscopy has been shown to be a better technique in detecting local symmetry changes as compared to pXRD which is very good in determining crystal structure for crystalline materials with well defined long range order [3]. It is clear that since bond energies are dependent on the bond properties, such

as bond constants and atom positions, the underlying thermodynamic properties will depend on the data provided by techniques that accurately reflect a local structure.

The controversies in explaining phase transitions related to space group information in $C_5H_5NHPF_6$ is analogous to the $LiPF_6$ case, which has been shown to display a possible cubic phase at local symmetry level using Raman spectroscopy, while the long range cooperative symmetry is a trigonal based structure according to XRD data [3]. The effect of this on $LiPF_6$ thermogravimetric data is profound, particularly when it comes to activation energy determinations, which are said to be reported with varying magnitudes [8]. This shows that a change in chemical composition or a possible phase transition, accompanied by a change in crystal structure of a material, will have an effect on the thermal properties of a substance.

In this work, we report the vibrational spectroscopy data of $C_5H_5NHPF_6$ as correlated to group theoretical works and we show that the space group *R-3m (166)* as reported in literature [6] is not an accurate reflection of the compound, but rather an *Fm3m (225)* space group is a more representative alternative. We further show the thermal decomposition kinetics of $C_5H_5NHPF_6$ and its thermal decomposition signature.

## 2. Experimental methods and materials

### 2.1 Synthesis of $C_5H_6NHPF_6$

A method proposed by Willmann *et al.* [9] for the synthesis of pyridinium hexafluorophosphate was used. Approximately 20 ml of aqueous $HPF_6$ acid was added to a beaker and stirred continuously. About 10ml of pyridine was added drop wise using a syringe while continuously stirring. The precipitate was filtered using a vacuum system and washed with water, and then the product was dried in an oven at 90 degrees Celsius for 6 hours.

## 2.2 Raman and infrared spectroscopy

The Ram II module (FT-Raman) mounted onto a vertex 70 FT-IR spectrometer (Bruker) was used to record the Raman spectra from 3500 to 0 $cm^{-1}$. The sample was in a solid form. A 1064 nm wavelength excitation radiation was used and a 50 mW power setting and a wavenumber resolution of 4 $cm^{-1}$ was used throughout this study. FT-ATR Infrared reflectance spectra for powder samples were recorded with a Tensor T27 FT-IR spectrometer fitted with a Harrick Mvp-pro ATR cell. All reflectance spectra were recorded between 4000 to 500 $cm^{-1}$ with 32 scans and a resolution of 4 $cm^{-1}$.

## 2.3 $^{13}C$ NMR analysis

For the $^{13}C$ NMR, a Bruker NMR Spectrometer 500 was used for the analysis. The instrument was set for $^{13}C$ dipolar dephasing (non-quaternary suppression) at room temperature (24.5 °C); $^{13}C$ NMR (126 MHz, Deuterated methanol solvent) δ 244.94, 236.46, 224.39, 149.36, 141.47, 128.90, 53.68, 45.99, 33.77.

## 2.4 Thermal decomposition

### *2.4.1 TG*

About 20 mg sample of $C_5H_5NHPF_6$ was analyzed on a modified TGS-2 Perkin Elmer TGA instrument. The instrument was enclosed within a dry glovebox and constantly purged with nitrogen gas. The sample was therefore heated from 30 to 600 °C at 10 °C/min under nitrogen purge gas.

### *2.4.2 Thermal decomposition reactor-IR system*

An in-house developed thermal decomposition reactor system coupled to a BOMEM MB 3000 spectrometer was used. The $C_5H_5NHPF_6$ salt was loaded into a Ni sample pan, fitted into a tube reactor and then purged with a constant flow of laser-grade helium. A Hi-Tech Elements heater was used to heat the stainless-steel tube reactor to 350 °C. The evolved

gas was captured at 20-minute intervals with an Infrared gas cell fitted with zinc selenide windows, and a spectrum was recorded.

### *2.4.3 Kinetic studies*

Decomposition kinetics studies were carried out using an isothermal method based on TG data obtained by using a dedicated TG instrument placed in a nitrogen glove box as in section 2.4.1. Experimentally obtained data was fitted into various solid state kinetic models tabulated in the ICTAC kinetics committee recommendations by Vyazovkin *et al*. [10] and the best line fit using the least squares statistical evaluation technique was chosen. A confidence interval of 95% (Table 3) was used.

The following integrated rate equation was used:

$$g(\alpha) = \left[1 - (1-\alpha)^{\frac{1}{3}}\right] = kt \qquad (1)$$

In Eq. (1), $\alpha$ is the extent of the reaction as derived from the global mass loss based on TG experimental data, $k$ is the rate constant ($s^{-1}$) and $t$ is time (s). The extent of the reaction is calculated using Eq. (2).

$$\alpha = \frac{m_0 - m_t}{m_0 - m_f} \qquad (2)$$

Where $m_0$ is the initial mass, $m_t$ is the mass at a particular time and $m_f$ is the final mass.

The dependence of the rate constant on temperature is based on the Arrhenius equation:

$$k = A\exp\left(\frac{-E_a}{RT}\right) \qquad (3)$$

Where $E_a$ is the activation energy in J.mol$^{-1}$, $R$ is the universal gas constant (8.314 J.mol$^{-1}$.K$^{-1}$) and $A$ is the pre-exponential factor (s$^{-1}$) associated with the rate of the reaction. The temperature $T$ has units in Kelvin. The value of the rate constant, $k$ at a particular temperature, was obtained from the slope of the *g(α) versus* time curve (Eq. 1).

## 3. Results and discussion

Raman and IR data of $C_5H_5NHPF_6$ in Figure 1a and b showing the vibrational band frequencies and their assignments are given in Table 1. The 551 and 795 cm$^{-1}$ IR active bands belong to $T_{1u}$ ($v_4$ and $v_3$ respectively). The $T_{1u}$ is the only IR active mode from the octahedral $PF_6^-$ anion in the compound; the others are contribution from the pyridinium ring. Previously, the vibrational band assignments for the $C_5H_5NHPF_6$ were done by Mohamed *et al* [2] and they were in line with the presence of an octahedral $PF_6$ anion in the molecule. The frequencies of these P-F bending and stretching modes are similar to other $MPF_6$ salts (M= $Li^+$, $Na^+$ and $K^+$) as reported by Kock *et al.* [3]. The normal modes of this ionic solid are a combination of those from the octahedral $PF_6$ structure and the ring breathing modes (Table 1) [2,7]. It is therefore important that the space group assigned to the $C_5H_5NHPF_6$ supports the presence of octahedral irreducible representations.

**Table 1: Here**

**Figure 1: Here**

The 1608 cm$^{-1}$ vibration splits into two, and when interpreted together with the broad nature of the 3326 cm$^{-1}$ band, vibrations associated with $H_2O$ can be said to be superimposed with the N-H and ring vibrations at these frequencies. This could indicate the presence of crystal water.

According to Copeland *et al* [6], the crystallographic space group for the compound $C_5H_5NHPF_6$ belong to *R-3m (166)* based on the single crystal x-ray determination. From

the basis of the space group data [6] and considering the relevant atomic equilibrium in the site symmetries, the crystallographic space group *R-3m (166)* can be correlated to a spectroscopic space group $D^5_{3d}$ [11]. Considering the full site symmetry associated with this space group, there are two distinct kinds of $D_{3d}$ sites, one accommodating one nitrogen atom and the other taking one phosphorus atom. The six hydrogens occupy a $C_2$ site, while the fluorine atoms occupy a $C_s$ site. The carbon atoms would split to occupy two different sites; one $C_{2h}$ site would accommodate three and then a $C_{3v}$ site would accommodate two carbon atoms. The total irreducible representations for this scenario would therefore be given in Equation 4 below.

$$\Gamma^{Total}_{C_5H_5NHPF_6} = 3A_{1g}^{(R)} + 5E_g^{(R)} + 8E_u^{(I)} + 5A_{2u}^{(I)} + 3A_{1u} \quad (4)$$

Therefore eight Raman active modes are expected, noting that five of them are doubly degenerate. In addition, thirteen IR active modes are expected, noting that eight of them are doubly degenerate. On the other hand, the $A_{1u}$ term is silent. Considering a three dimensional solid material, there are *3N-3* number of vibrations expected, and this would translate into 54 vibrations for a 19 atom compound like $C_5H_5NHPF_6$ (with $Z^B = 1$ and N = 19), which is clearly incompatible with the 37 total vibrations predicted by Equation 4. Based on this explanation, and taking into account that there is no single $T_{1u}$ mode predicted by Equation 4, an inherent part of a $PF_6$ anion octahedral structure [2,3,4], the space group for $C_5H_5NHPF_6$ may not be interpreted as *R-3m (166)* based on group theory and vibrational spectroscopy data.

The understanding of the orientation of the $PF_6^-$ anion relative to the pyridinium ring becomes important in order to better predict a correct crystal structure for $C_5H_5NHPF_6$. Solid state $^{13}C$ NMR of pyridinium hexafluorophosphate is shown in Figure 2a. The NMR spectrum indicates three significant signals corresponding to the three chemical environments expected on a pyridinium ring i.e. γ (8C and 12C), β (11C and 9C) and α (10C) carbons as shown in Figure 2b.

**Figure 2a: Here**
**Figure 2b: Here**

A signal at δ = 149.36 ppm, integrating for one carbon, correlates with the γ carbon on the ring. The signal at δ = 141.47 ppm integrating for two carbons corresponds to the two α carbons of the pyridinium ring, the two α carbons appear at such a high chemical shift of δ = 141.47 ppm due to the deshielding effect from the electron withdrawing hexafluorophosphate ion. Finally the signal at δ = 128.90 ppm integrating for two carbons is representative of the two β carbons of the pyridinium ring. It should be noted that the lack of resolution resulting in the broadening of signals is the results of solid state run NMR, hence poor splitting. From the NMR data in Figure 2 and Table 2, the presence of a pyridinium ring and $PF_6^-$ anion in the synthesized compound are confirmed.

**Table 2: Here**

The prediction of three chemically different carbon atoms by $^{13}C$ NMR means that the hexafluorophosphate anion must be symmetrical with respect to the pyridinium ring's $C_{2v}$ symmetry, with monodentate coordination between the anion's fluorine atom and the positive point charge at the nitrogen position of the ring. In this configuration, the most significant consideration to bear in mind is that the pyridinium ring appears as a positive point charge relative to the $PF_6$ anion, an arrangement analogous to other $MPF_6$ salts (M= Li, Na, K). These inorganic $MPF_6$ salts have been shown to belong to an *Fm3m (225)* space group by kock *et al.* [3]. Taking this view into account, and therefore assuming an *Fm3m (225)* space group for $C_5H_5NHPF_6$, we obtain the following irreducible representations based on group theory calculations (Equation 5):

$$A_{1g}^{(R)} + E_g^{(R)} + T_{2g}^{(R)} + 12T_{1u}^{(I)} + T_{1g}^{(s)} + 3T_{2u}^{(s)} \qquad (5)$$

Equation 5 predicts 54 vibrations for $C_5H_5NHPF_6$, noting that 6 of them are Raman active with subscript (R), 36 are infrared active (I) and 12 of them are silent (S). It is therefore better to represent the crystal structure of $C_5H_5NHPF_6$ as a cubic *Fm3m (225)*, consistent with the assignments of an octahedral $PF_6$ anion from Mohamed *et al* [2] for the same compound.

Further evidence of a cubic related structure for $C_5H_5NHPF_6$ comes from Raman and infrared data (Figure 1). The $T_{1u}$ band at 111 $cm^{-1}$ is inherently an IR active mode but appears in Raman spectra. Its appearance in the Raman spectra of $C_5H_5NHPF_6$, together with $A_{1g}$ appearing in the IR spectra, is a sign of a break in the centrosymmetric geometry of the molecule and thus points to a distortion in the $PF_6$ anion. This behavior has been observed in other hexafluorophosphate salts such as the $LiPF_6$ by Kock *et al* [3] with a $T_{1u}$ band appearing at 99 $cm^{-1}$ and also at 76 $cm^{-1}$ for $CsPF_6$ as observed by Heyns *et al* [18], which are all cubic compounds within the space group *Fm3m* (225).

The space group information has direct influence on the thermodynamic properties of the material. In order to understand the decomposition profile of $C_5H_5NHPF_6$, the material was subjected to a strictly anhydrous environment (section 2.4.2), and thermally decomposed into its gaseous components. The composition of the thermal decomposition off-gas products shows presence of crystal water in the pyridinium hexafluorophosphate sample. This follows from the fact that the thermal decomposition reactor, the sample powder and the lines were thoroughly purged with pure $PF_5$ gas until no traces of hydrolysis products were observed prior to thermal decomposition of $C_5H_5NHPF_6$. However, the IR spectrum of the off-gas products (Figure 3) shows bands at 1416, 993 and 868 $cm^{-1}$, in line with the values reported by Yang *et al*. [12] for $POF_3$. Hydrogen fluoride is also observed at 3884 $cm^{-1}$ as expected. Although $PF_5$ gas was expected as a product according to Equation 5, it is known that in the presence of water, $POF_3$ evolves as a by-product [13]. Following the argument on the basis of the experimental procedure to eradicate moisture in the system, and considering possible existence of water according to IR spectrum in Figure 1b, a possible source of water would therefore be in the form of crystal water, which would be an intricate part of the compound.

The intense vibrational bands associated with the strong IR absorber, the $POF_3$ gas, suppresses the observed intensity of pyridinium ring vibrational bands at 1157 and 1298 $cm^{-1}$.

**Figure 3: Here**

$$C_5H_5NHPF_6 \xrightarrow{\Delta} C_5H_5N + HF + PF_{5(g)} \quad (6)$$

$$PF_{5(g)} + H_2O_{(g)} \rightarrow POF_{3(g)} + 2HF_{(g)} \quad (7)$$

The TG profile of $C_5H_5NHPF_6$ is presented in Figure 4. The onset of thermal decomposition of $C_5H_5NHPF_6$ is 125 °C. Only 0.24% of the substance remains as non volatile material, which could essentially just be impurities (Figure 4).

**Figure 4: Here**

Several models were evaluated for the thermal decomposition study of pyridinium hexafluorophosphate (Table 3). Based on the best line fit of 99.98%, the compound $C_5H_5NHPF_6$ was found to thermally decompose according to the contracting volume model (R3, three dimensional), giving off HF and pyridine, with the observed $POF_3$ as a byproduct of $PF_5$ gas (Figure 3).

**Table 3: Here**

**Figure 5: Here**

The activation energy ($E_a$) for the thermal decomposition reaction of $C_5H_5NHPF_6$ is found to be 108.5 ($kJ.mol^{-1}$), which is of similar magnitude as that of the $LiPF_6$ reported

to be 116.0 kJ.mol$^{-1}$ [8]. Furthermore, compared to the $LiPF_6$, there is a higher fraction of collisions for the $C_5H_5NHPF_6$ as indicated by an increased frequency factor during thermal decomposition; a pre exponential factor value (*A*) of 1.51 x $10^9$sec$^{-1}$ is obtained. This means that the thermal decomposition of $C_5H_5NHPF_6$ is highly favoured.

## 4. Conclusion

Thermal decomposition and vibrational spectroscopic properties of pyridinium hexafluorophosphate have been presented, and based on vibrational spectroscopy, the results support a space group *Fm3m (225)* as opposed to the previously proposed *R-3m (166)*. The conclusions were drawn based on the vibrational spectroscopic experiments and correlation data between the site symmetry and spectroscopic space group of the same compound. The $^{13}$C NMR of the pyridinium hexafluorophosphate indicates a deshielding effect from the electron withdrawing hexafluorophosphate anion, showing strong influence of the anion's fluorine atoms on alpha carbons. Furthermore, the data indicates three significant signals corresponding to the three chemical environments expected on a pyridinium ring i.e. γ, β and α carbons, suggesting that the anion must be symmetrical with respect to the pyridinium ring's $C_{2v}$ symmetry, with a monodentate coordination. The thermal decomposition of the compound follows a contracting volume model, with activation energy of 108.5 kJ.mol$^{-1}$ and a pre exponential factor of 1.51 x $10^9$sec$^{-1}$.

**ACKNOWLEDGEMENTS**

The South Africa Nuclear Energy Corporation Soc. Ltd and the Fluorochemical Expansion Initiative (FEI) program of the Department of Science and Technology (Republic of South Africa) are greatly acknowledged for their funding for the PhD study. The University of Pretoria is acknowledged for PhD studies. We also acknowledge Benni Vilakazi for assistance with experiments and Lindani Ngidi for NMR data review.

## REFERENCES

[1] A.T. Balaban, D. Mateescu, M. Elian, Infrared absorption spectra of pyrylium salts, Tetrahedron 18 (1962) 1083-1094.

[2] K.S. Mohamed, D.K. Padma, Spectral studies on pyridinium hexafluorophosphate, Spectrochim. Acta A 41A (1985) 725-728.

[3] L.D. Kock, M.D.S. Lekgoathi, P.L. Crouse, B.M. Vilakazi, Solid state vibrational spectroscopy of anhydrous lithium hexafluorophosphate, J. Mol. Struct. 1026 (2012) 145-149.

[4] M.D.S. Lekgoathi, L.D. Kock, Effect of short and long range order on crystal structure interpretation: Raman and powder X-ray diffraction of $LiPF_6$, Spectrochim. Acta A 153 (2016) 651-654.

[5] M. Hanaya, N. Ohta, M. Ogijni, Calorimetric study of phase transitions in pyridinium iodide and pyridinium hexafluorophospate crystals, J. Phys. Chem. Solids 54 (1993) 263-269.

[6] R.F. Copeland, S.H. Conner, E.A. Meyers, The crystal structures of the pyridinium salts of the group Vb. hexafluoride anions, J. Phys. Chem. 70 (1996) 1288-1296.

[7] R. Cook, Vibrational spectra of pyridinium salts, Can. J. Chem. 39 (1961) 2009-2024.

[8] M.D.S Lekgoathi, B.M. Vilakazi, J.B. Wagener, J.P. Le Roux, D. Moolman, Decomposition kinetics of anhydrous and moisture exposed $LiPF_6$ salts by thermogravimetry, J. Fluorine Chem. 149 (2013), 53-56.

[9] P. Willmann, R. Naejus, R. Coudert, D. Lemordant, Solvate of Lithium Hexafluorophosphate and Pyridine, Its preparation and Preparation Process for Lithium Hexafluorophosphate Using Said Solvate, US Patent 5,993,767 (1999), 1-7.

[10] S.Vyazovkin, A.K. Burnham, J.M. Criado, L.A. Perez-Maqueda, C. Popescu, N. Sbirrazouli, ICTAC kinetic committee recommendations for performing kinetic computations on thermal analysis data, Thermochim. Acta 520 (2011) 1-19.

[11] W.G. Fateley, F.R. Dollish, N.T. McDevitt, F.F. Bentley, Infrared and Raman Selection rules for Molecular and Lattice Vibrations: The Correlation Method, Wiley-Interscience, New York (1972) 1-220.

[12] H. Yang, G.V. Zhuang, P.N. Ross Jr, Thermal stability of $LiPF_6$ salt and Li-ion battery electrolytes containing $LiPF_6$, J. Power Sources 161 (2006), 573-579.

[13] T. Kawamura, S. Okada, J. Yamaki, Decomposition of $LiPF_6$-based electrolytes for lithium ion cells J. Power Sources, 156 (2006) 547-554.

[14] A.C. Doriguetto, T.M. Boschi, P.S. Pizani, Y.P. Mascarenhas J. Ellen, The effect of the cation substitution on the structural and vibrational properties of $Cs_2NaGaxSc1ÀxF_6$ solid solution, J.Chem. Phys. 121 (2004) 3184-3190.

[15] A.B. Campos, A.Z. Simoes, E. Longo, J.A. Varela, V.M. Longo, A.T. de Figueiredo, F.S. De Vincente A.C. Hernades, Mechanisms behind blue, green, and red photoluminescence emissions in CaWO4 and CaMoO4 powders, Appl. Phys. Lett. 91 (2007), 0519231-05192313.

[16] A. Aroca, M. Nazri, A.J. Camargo, M. Trsic, Vibrational spectra and ion-pair properties of lithium hexafluorophosphate in ethylene carbonate based mixed-solvent systems for lithium batteries, J. Solution Chem. 29 (2000) 10.

[17] K. Nakamoto, Infrared and Raman spectra of inorganic and coordination compounds, Part A: Theory and applications in inorganic chemistry, Wiley, 6th Edition, (2009) 222-223.

[18] A.M. Heyns, P.W. Richter, J.B. Clark, The vibrational spectra and crystallographic properties of CsPF6, J. Solid State Chem. 39 (1981) 106–113.

## List of Figure Captions

Figure 1: Raman spectrum of $C_5H_5NHPF_6$ (a) and FTIR-ATR spectrum of $C_5H_5NHPF_6$ (b).

Figure 2a: A $^{13}C$ NMR spectrum and chemical structure depiction of $C_5H_5NHPF_6$ compound

Figure 2b: Graphical representation of the relative positions of the two ions in the $C_5H_5NHPF_6$

Figure 3: IR spectrum of gaseous decomposition products of $C_5H_5NHPF_6$ under helium atmosphere

Figure 4: TG curve of $C_5H_5NHPF_6$ sample heated under dry nitrogen from 30 to 600°C

Figure 5: A plot of lnK vs 1/T for thermal decomposition of solid $C_5H_5NHPF_6$

Table 1: FTIR vibrational spectra of $C_5H_5NHPF_6$.

| **Reference ($cm^{-1}$)** | **Assignment** | **This work ($cm^{-1}$)** |
|---|---|---|
| 471,475,478[4] | $T_{2g}$ Octahedral | 475 |
| 571, 579, 586[4] | $E_g$ Octahedral | 643 |
| 558[2], 551[17] | $T_{1u}$ Octahedral | 551 |
| 670[2],680[7] | $A_1$, Ring vibrations | 668 |
| 745[17],738[16] | Ring breathing mode | 735 |
| 830[2] | $A_{1g}$ Octahedral | 795 |
| 1490[2],1540[2], 1481[7] | $B_1$ Ring vibrations | 1490,1540 |
| 1585[2],[7] | $A_1$ Ring vibrations | 1608 |
| 3236[7] | $A_1$ Ring vibrations | 3326 |

Observed = this work.

Table 2: A $^{13}C$ NMR data of solid $C_5H_5NHPF_6$.

| Observed shift | *Reported shift | Ring Carbons |
|---|---|---|
| 141.47 | 141.97 | 2 α |
| 128.90 | 127.25 | 2 β |
| 149.36 | 146.43 | 1-γ |

*Mohamed and Padma, (1985).

Table 3: Comparison of the three closest models that best fit TG experimental data.

| Model | Description | Equation |
|---|---|---|
| R2 | Contracting area | $g(\alpha) = \left[1 - (1-\alpha)^{\frac{1}{2}}\right] = kt$ |
| R3 | Contracting volume | $g(\alpha) = \left[1 - (1-\alpha)^{\frac{1}{3}}\right] = kt$ |
| D1 | 1-D diffusion | $g(\alpha) = [(\alpha)^2] = kt$ |

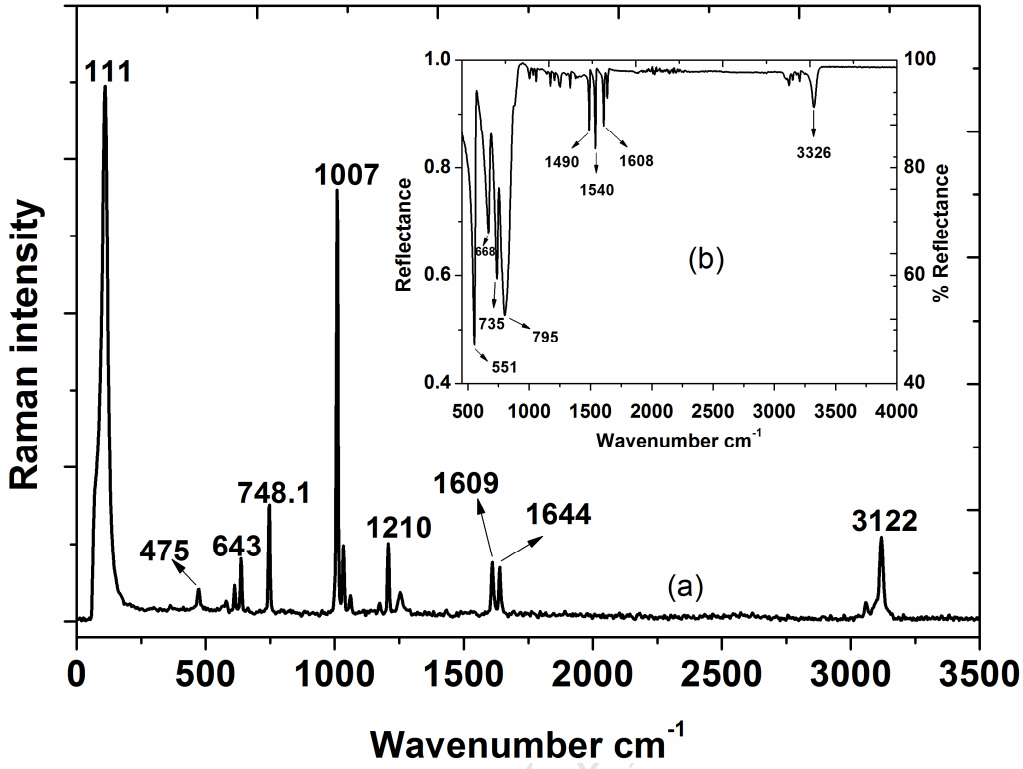

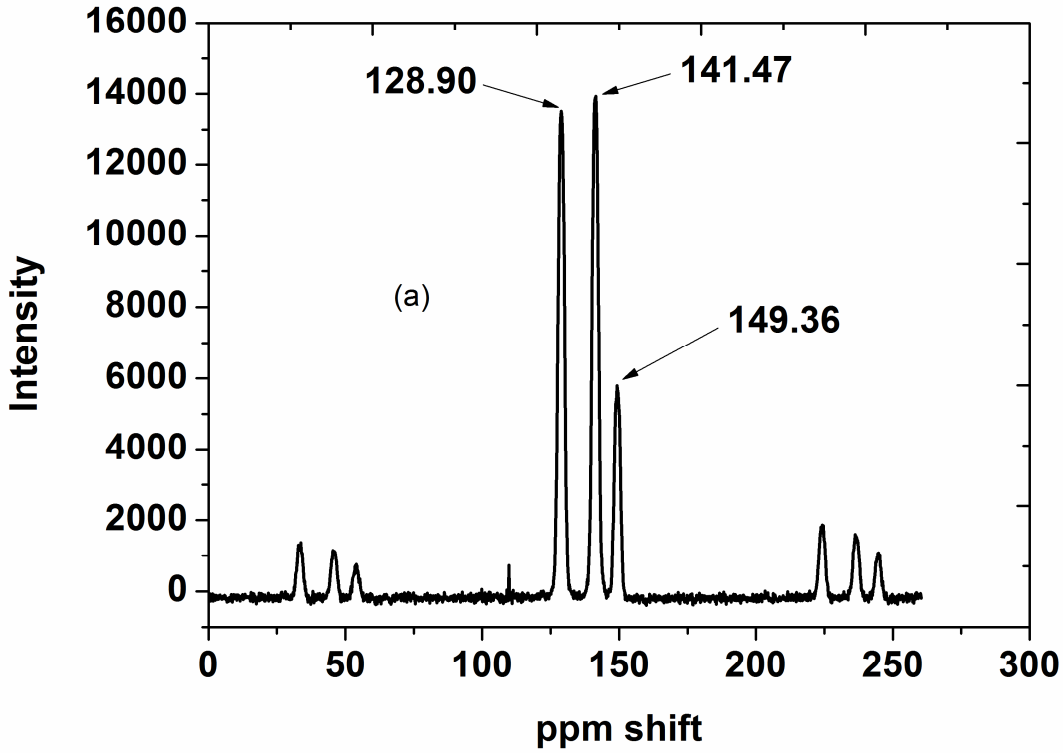

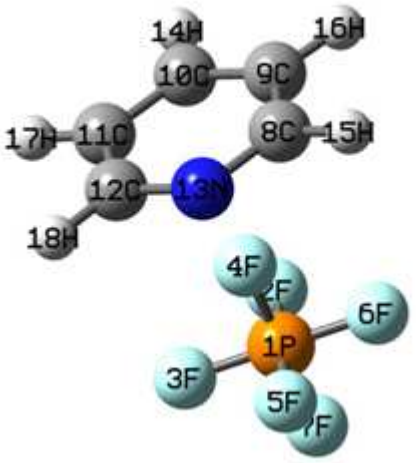

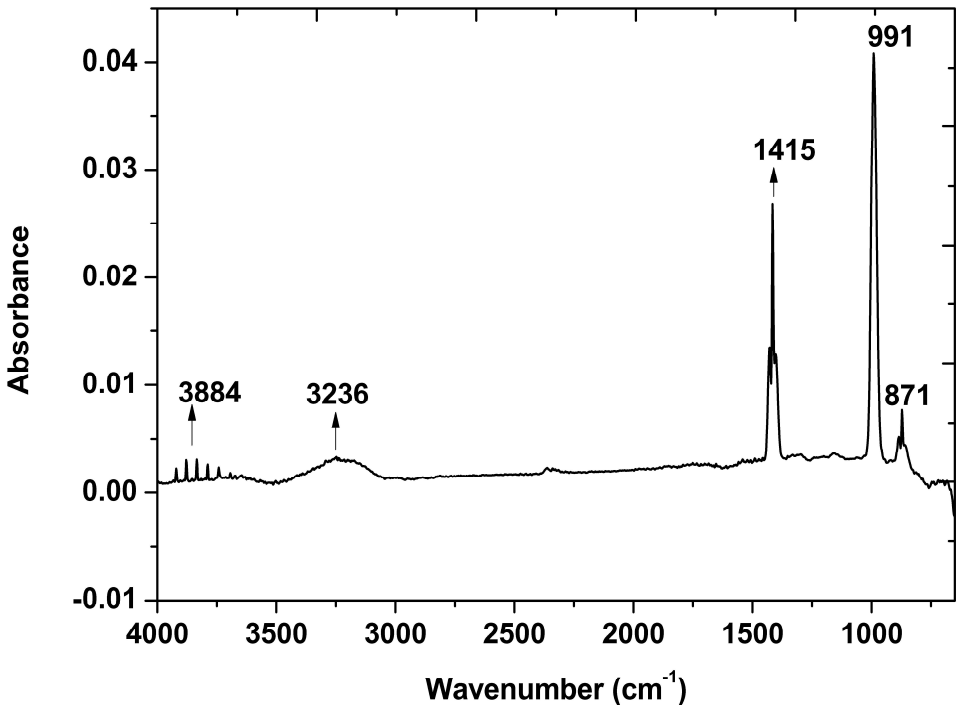

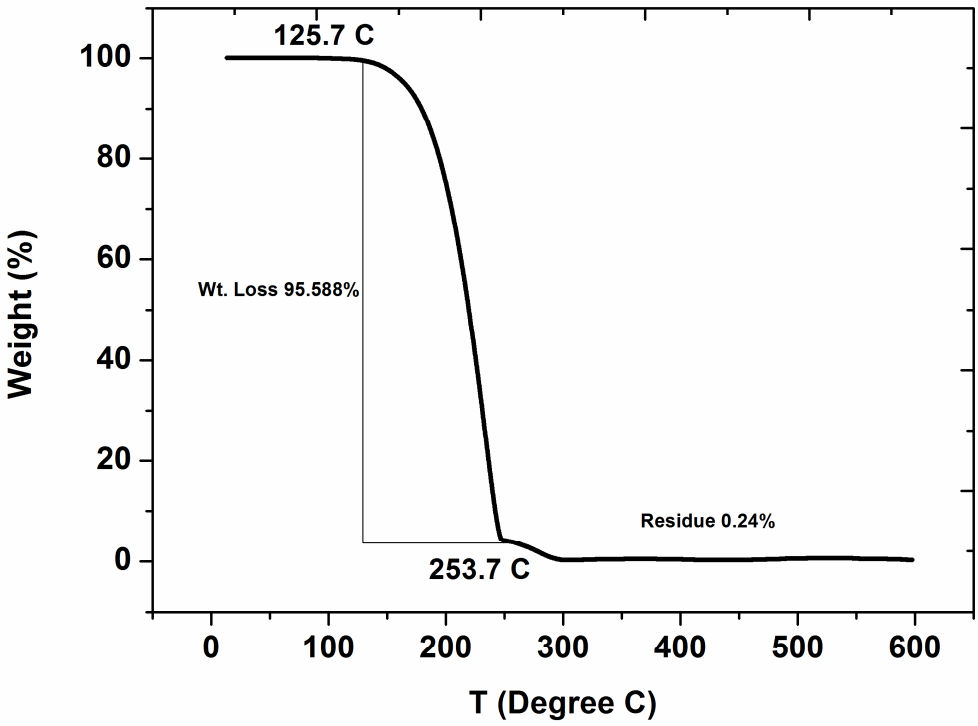

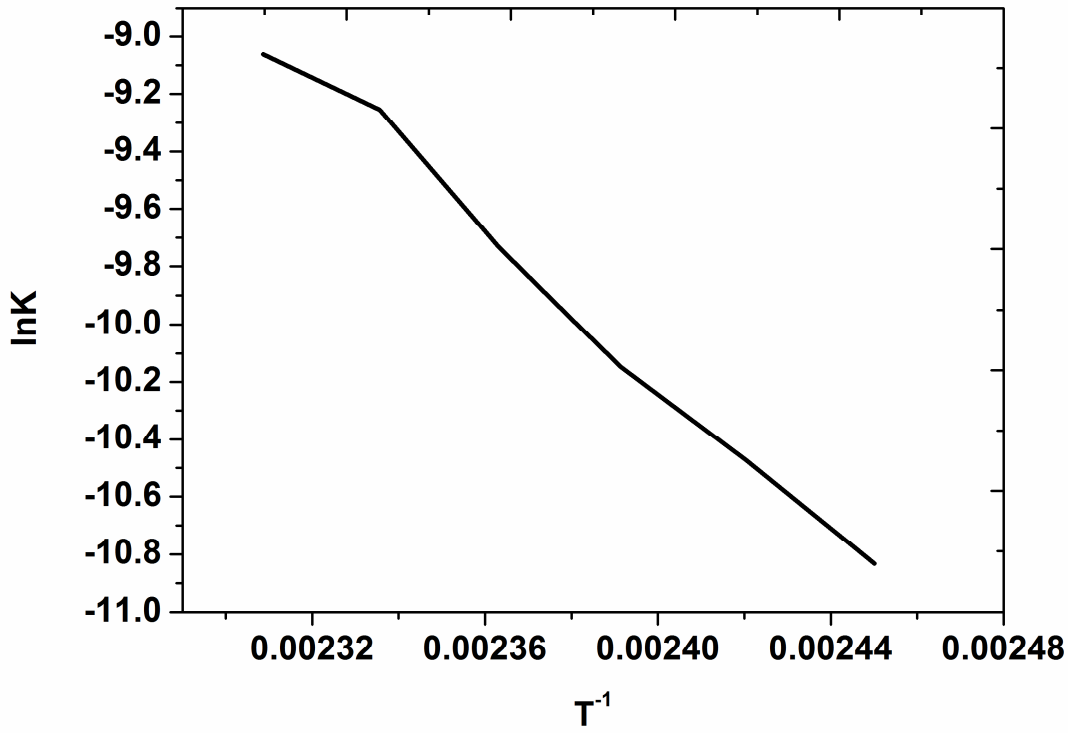

## Highlights

- Vibrational spectroscopy of $C_5H_5NHPF_6$ correlated to group theory is presented.
- The space group for $C_5H_5NHPF_6$ is not *R-3m(166)* as previously thought.
- The $^{13}C$ NMR data supports vibrational spectroscopy space group calculations.
- The $PF_6^-$ anion is symmetrical with respect to the pyridinium ring's $C_{2v}$ symmetry.
- Therefore $C_5H_5NHPF_6$ is better interpreted as having cubic space group *Fm3m (225)*.